

Multi-scale theory in the molecular simulation of electrolyte solutions

W. Zhang,^{1, a)} X. You,^{1, b)} and L. R. Pratt^{1, c)}

Department of Chemical and Biomolecular Engineering, Tulane University, New Orleans, LA 70118

This paper organizes McMillan-Mayer theory, the potential distribution approach, and quasi-chemical theory to provide theory for the thermodynamic effects associated with longer spatial scales involving longer time scales, thus helping to define a role for AIMD simulation directly on the time and space scales typical of those demanding methods. The theory treats composition fluctuations which would be accessed by larger-scale calculations, and also longer-ranged interactions that are of special interest for electrolyte solutions. The quasi-chemical organization breaks-up governing free energies into physically distinct contributions: *packing*, *outer-shell*, and *chemical* contributions. Here we study specifically the *outer-shell* contributions that express electrolyte screening. For that purpose we adopt a primitive model suggested by observation of ion-pairing in tetra-ethylammonium tetra-fluoroborate dissolved in propylene carbonate. Gaussian statistical models are shown to be effective physical models for *outer-shell* contributions, and they are conclusive for the free energies within the quasi-chemical formulation. With the present data-set the gaussian physical approximation obtains more accurate mean activity coefficients than does the Bennett direct evaluation of that free energy.

I. INTRODUCTION

This paper develops statistical mechanical theory with the goal of treating electrolyte solutions at chemical resolution. Our context is current research on electrochemical double-layer capacitors (EDLCs) based on nanotube forests.¹ The requirement of chemical resolution means that electronic structure must be an integral part of the theory consistent with the natural interest in chemical features of EDLCs.

Ab initio molecular dynamics (AIMD), though not statistical mechanical theory, is available to simulate electrolyte solutions. Compared to classic molecular simulations with empirical model force-fields, AIMD calculations are severely limited in space and time scales, by more than an order-of-magnitude in each. Consequently, application of AIMD is not feasible for EDLCs at scales

that are experimentally interesting. This calls for further theory to embed AIMD methods in studies of EDCLs.

Change-of-scale consequences are a primitive goal of fundamental statistical mechanical theory. That basic perspective is explicit in the classic phase transition literature,² and it has long been relevant to the theory of electrolyte solutions specifically.^{3,4} This paper organizes several basic results of the statistical mechanics of solutions to treat electrolyte solutions where space and time scales will otherwise prohibit direct AIMD calculations. Our results here suggest a role for AIMD somewhat analogous to sub-grid modeling in computational fluid mechanics. Nevertheless, the goals of the statistical thermodynamics of complex solutions are distinct, and we do not propose transfer of results here between those fields.

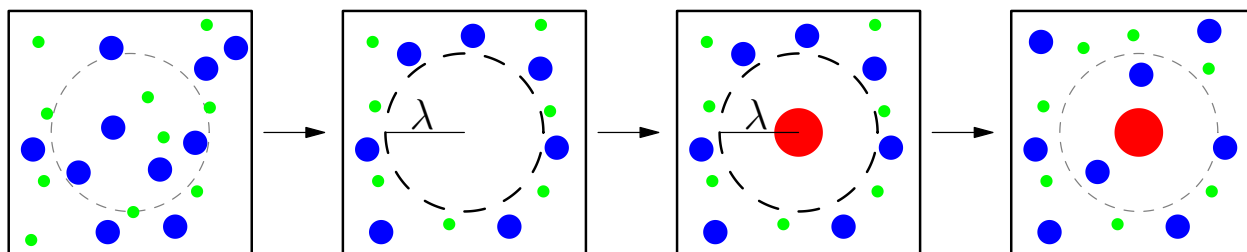


FIG. 1. Evaluation of the excess chemical potential of a distinguished ion (red disk), patterned according to QCT. The blue and green disks are other ions in the system, and the solvent is in the background. The stepwise contributions are “packing,” “outer shell,” and “chemical” contributions, from left to right. See the text and Eq. (11) for further discussion.

^{a)}Electronic mail: wzhang4@tulane.edu

^{b)}Electronic mail: xyou@tulane.edu

Our development here utilizes several theoretical results that are "... both difficult and strongly established ..."³ We put burdensome technical results in appendices, and in this introduction give a fuller discussion of the line of reasoning.

The initial step in our development is the McMillan-Mayer (MM) theory^{3,5,6} *integrating out* of solvent degrees of freedom. MM theory is a pinnacle of coarse-graining for the statistical mechanics of solutions, all primitive models rest on it, and it achieves a vast conceptual simplification the theory of electrolyte solutions. No sacrifice of molecular realism is implied by MM theory. But cataloging the multi-body potentials required for a literal MM application is prohibitive.⁷ Therefore, use of MM theory to construct a specific primitive model for a system of experimental interest has been limited.^{8,9} Indeed, the MM theory is not generally suitable for specific molecular-scale implementation.

To address this we exploit *quasi-chemical theory* (QCT) which is formally complete in its modern expression.^{10,11} QCT evaluates solvation free energies by breaking them into contributions with clear physical meanings. One contribution is a *packing* contribution. This can be simple in the anticipated applications because the solvent is not involved specifically, and the ion concentrations are not prohibitively high. A second contribution — the *outer shell* contribution — treats ion-ion interactions at long-range and it is expected on physical grounds that the necessary MM interactions should be simple then. That outer-shell contribution is studied below.

The final contribution — the *chemical* contribution — treats ion-ion inner-shell neighbors. Smaller spatial scales must be directly confronted and it is here that the sub-grid AIMD activity comes into play. Fig. 1 shows a now-standard picture of this organization of the statistical thermodynamical problem.

This discussion suggests that van der Waals theory is a subset of the present QCT approach. This is advantageous because van der Waals theory is the basis of the theory of liquids viewed broadly.^{12,13} While paying an unavoidable price of significant computational effort, QCT goes beyond van der Waals theory in several ways. For example here, where ion-pairing is an essential part of the physical picture, associative phenomena are treated fully. Furthermore, our QCT implementation would routinely treat outer-shell interactions through gaussian order rather than the mean-field approach of classic van der Waals theories. This is essential in the present applications in order to capture the physical effect of Debye screening of ion correlations.

It is an interesting physical point that the identification of *packing* and *chemical* contributions here is a con-

sequence of a choice of conditioning event, in the present development the emptiness of the inner-shell. This has the advantages that the theory is a close relative of van der Waals theory, and that the outer-shell contribution should be particularly simple to evaluate. But other choices of conditioning event are possible too.¹⁴ For example, the conditioning event might be the event that the occupancy of the inner-shell is the value most probably observed. This has the intuitive attraction of being close to simple observations. But it presents the challenge that the evaluation of the partition function for that case might be more difficult. In what follows, our primary emphasis is to characterize the computational effort to evaluate the partition function associated with *outer-shell* contribution that arises with the original suggestion for the conditioning event.

The plan of this paper is as follows: Sec. II records several theoretical specifics that are required for our argument. The Appendix A gives an accessible derivation of the MM theory results used here; Appendices B and C present technical features of the Potential Distribution Theory and Quasi-Chemical Theory, respectively, required in the main text. Sec. III gives a demonstration of the results obtained for a primitive electrolyte solution model that was designed to correspond to the tetra-ethylammonium tetra-fluoroborate in propylene carbonate (TEABF₄/PC) where ion-pairing can be important.¹⁵

II. BASIC THEORY REQUIRED

A. McMillan-Mayer theorem

The osmotic pressure, π , is evaluated as the partition function

$$e^{\beta\pi V} = \sum_{\mathbf{n}_A \geq 0} \mathcal{Z}(\mathbf{n}_A; \mathbf{z}_S) \left(\frac{\mathbf{z}_A^{\mathbf{n}_A}}{\mathbf{n}_A!} \right), \quad (1)$$

involving only the solute species A. Here V is the volume, $k_B T = \beta^{-1}$ the temperature, and the activity of the solvent (species S) is denoted by $\mathbf{z}_S = e^{\beta\mu_S}$. Eq. (1) involves

$$\mathcal{Z}(\mathbf{n}_A; \mathbf{z}_S) = \left[\lim_{\mathbf{z}_A \rightarrow 0} \left(\frac{\rho_A}{\mathbf{z}_A} \right)^{\mathbf{n}_A} \right] \times \int_V d\mathbf{1}_A \dots \int_V d\mathbf{n}_A e^{-\beta W(\mathbf{1}_A \dots \mathbf{n}_A)}, \quad (2)$$

with ρ_A being the density of solutes, and with the potentials-of-average-force given by

$$W(\mathbf{1}_A \dots \mathbf{n}_A) = -\frac{1}{\beta} \ln g(\mathbf{1}_A \dots \mathbf{n}_A; \mathbf{z}_S, \mathbf{z}_A = 0), \quad (3)$$

which depends on the the activity of the solvent. The result Eq. (2) is compact, thermodynamically explicit, and general; see the Appendix for an accessible derivation and fuller discussion.

^{c)}Electronic mail: lpratt@tulane.edu

B. Potential distribution theorem (PDT)

The solute chemical potential may be expressed as

$$\beta\mu_A = \ln \rho_A \Lambda_A^3 / q_A^{(\text{int})} + \beta\mu_A^{(\text{ex})} (z_A = 0) - \ln \left\langle \left\langle e^{-\beta\Delta W_A^{(1)}} \right\rangle \right\rangle_0. \quad (4)$$

The binding energy of a distinguished solute (A) molecule in the MM system is

$$\Delta W_A^{(1)} = W(\mathbf{n}_A + 1) - W(\mathbf{n}_A) - W(1). \quad (5)$$

The middle term of Eq. (4),

$$\beta\mu_A^{(\text{ex})} (z_A = 0) = -\ln \left\langle \left\langle e^{-\beta\Delta U_A^{(1)}} \right\rangle \right\rangle_0, \quad (6)$$

is evaluated at infinite dilution of the solute. This evaluation is typically highly non-trivial, but much has been written about that^{10,11} and we will proceed to analyze that right-most term of Eq. (4).

C. Quasi-chemical theory

Thus we study

$$\beta\Delta\mu_A^{(\text{ex})} = \beta\mu_A^{(\text{ex})} - \beta\mu_A^{(\text{ex})} (z_A = 0) = -\ln \left\langle \left\langle e^{-\beta\Delta W_A^{(1)}} \right\rangle \right\rangle_0. \quad (7)$$

$\Delta\mu_A^{(\text{ex})}$ is the contribution to the chemical potential of species A in excess of the infinite dilution result, due to inter-ionic interactions with the influence of solvent fully considered.

A quasi-chemical development of Eq. (7) starts by characterizing neighborhood. If the species considered are ions in solution, then we need to characterize ion neighbors of each ion in solution, distinguished in turn. Pairing of oppositely charged ions has been the subject of classic scientific history¹⁵ that can inform the present discussion. Pairing of tetra-fluoroborate 1-hexyl-3-methylimidazolium in pentanol has recently been studied both experimentally and computationally.¹⁶

Pairing of tetra-ethylammonium tetra-fluoroborate in propylene carbonate is a helpful example.¹⁵ In that case, pairing is simple to observe for saturated solution conditions and formation of chains and rings of ions is consistent with the molecular-scale observations. We might consider an indicator function χ_{AB} with the requirement that $\chi_{AB} = 1$ indicates *no* B ions are within an inner-shell stencil of a distinguished A ion. The simplest possibility, natural for compact molecular ions, is to identify a central atom in A and in B ions, and to set $\chi_{AB} = 1$ (but zero otherwise), when those atoms of further apart than a designated distance λ_{AB} .

Even simpler, and satisfactory for the primitive model that follows below, we might identify a central atom for

ion A, then define a spherical inner-shell by the radius λ_A with the requirement that *no* other ions be closer than that. In fact, we choose the same radius for cations and anions in the primitive model studied below, $\lambda_A = \lambda_A = \lambda$.

Eq. (7) was derived using the grand canonical ensemble. But implementation with simulations in the grand canonical ensemble would be painful. Calculations with *canonical* ensemble methods should be satisfactory. In what follows we will develop Eq. (7) from the perspective on the canonical ensemble. Appendix C discusses the relevant ensemble differences.

The canonical ensemble average of $e^{\beta\Delta W_A^{(1)}} \chi_A$ gives

$$\begin{aligned} \left\langle e^{\beta\Delta W_A^{(1)}} \chi_A \right\rangle &= \frac{\left\langle \left\langle e^{-\beta\Delta W_A^{(1)}} e^{\beta\Delta W_A^{(1)}} \chi_A \right\rangle \right\rangle_0}{\left\langle \left\langle e^{-\beta\Delta W_A^{(1)}} \right\rangle \right\rangle_0} \\ &= e^{\beta\Delta\mu_A^{(\text{ex})}} \langle \chi_A \rangle_0. \end{aligned} \quad (8)$$

In addition, for indicator function χ_A , and some other quantity G we have

$$\langle G\chi_A \rangle = \langle G | \chi_A = 1 \rangle \langle \chi_A \rangle. \quad (9)$$

Collecting these relations yields

$$e^{\beta\Delta\mu_A^{(\text{ex})}} = \left\langle e^{\beta\Delta W_A^{(1)}} | \chi_A = 1 \right\rangle \times \frac{\langle \chi_A \rangle}{\langle \chi_A \rangle_0}. \quad (10)$$

After evaluating the logarithm and replacing the conditional ensemble average with an integral over a conditional probability distribution, we get

$$\begin{aligned} \beta\Delta\mu_A^{(\text{ex})} &= -\ln \langle \chi_A \rangle_0 \\ &+ \ln \int e^{\beta\varepsilon} P_A(\varepsilon | \chi_A = 1) d\varepsilon + \ln \langle \chi_A \rangle \end{aligned} \quad (11)$$

where

$$P_A(\varepsilon | \chi_A = 1) = \left\langle \delta(\varepsilon - \Delta W_A^{(1)}) | \chi_A = 1 \right\rangle. \quad (12)$$

These three terms correspond to the three processes in Fig. 1.

III. NUMERICAL DEMONSTRATION

We have tested how Eq. (11) works numerically on the basis of a primitive electrolyte solution model that was designed to correspond to the TEABF₄/PC. Table I describes the model further and indicates the thermodynamic states studied by Monte Carlo calculations. The radial distribution functions (Fig. 2) show why this primitive model, with non-additive hard-sphere interactions, was identified to study ion-pairing.

In this case, the packing and chemistry contributions can be directly calculated by trial insertions (for *packing* and $\langle \chi_A \rangle_0$), and observation of the closest neighbor molecule distance distribution (for *chemistry* and $\langle \chi_A \rangle$).

c (mol/dm ³)	L (nm)	$n_{\text{ion-pairs}}$	κ^{-1} (nm)	$\beta q^2 \kappa / 2\epsilon$
0.01	32.15	200	2.67	0.17
0.05	18.80	200	1.19	0.39
0.1	14.92	200	0.84	0.55
0.2	11.84	200	0.60	0.77
0.4	9.4	200	0.42	1.11
0.5	9.4	250	0.37	1.26
0.6	9.4	300	0.34	1.37
0.8	9.4	400	0.30	1.55
1.0	9.4	500	0.27	1.72
2.0	7.4	500	0.19	2.44

TABLE I. Specifications for Monte Carlo simulation of a primitive model with dielectric constant, ion charges and sizes corresponding to the atomically detailed [TEA][BF₄]/PC case.¹⁵ Specifically the model dielectric constant is $\epsilon = 60$, and $d_{++} = 0.6668$ nm, $d_{--} = 0.6543$ nm, $d_{-+} = 0.45$ nm are distances of closest approach for the hard spherical ions. These calculations utilized the Towhee¹⁷ package adapted to the present system, conventional cubical periodic boundary conditions at $T = 300$ K, and the indicated concentrations c . Each calculation was extended to 10^6 cycles after aging, each cycle comprising $2n_{\text{ion-pairs}}$ attempted moves. 10,000 configurations are saved and used for the following analyses.

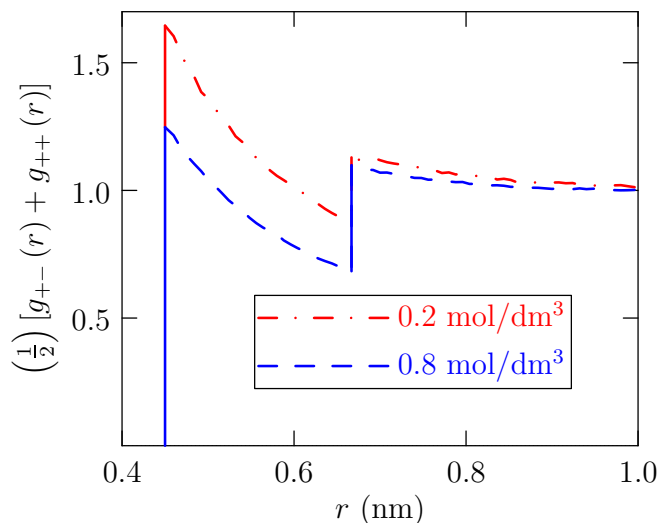


FIG. 2. The radial distribution functions of $c = 0.2$ mol/dm³ and $c = 0.8$ mol/dm³ from cation to other ions. These two vertical lines identify the closest approach distances, which are 0.45 nm and 0.6668 nm in this case.

That leaves the *outer-shell* contribution which is our particular interest here.

For the general theory (Eq. (11) and Fig. 1), the distinguished ion will be separated by a substantial distance from all other ions. We assume that the required binding energy can be approximated as a superposition of the pair potential-of-mean-force at long-range between the distinguished ion and all ion neighbors, which we take to be the classic macroscopic result $q_i q_j / 4\pi\epsilon r$ for a separation of r . That superposition is just the electrostatic inter-ionic potential energy of interaction for the

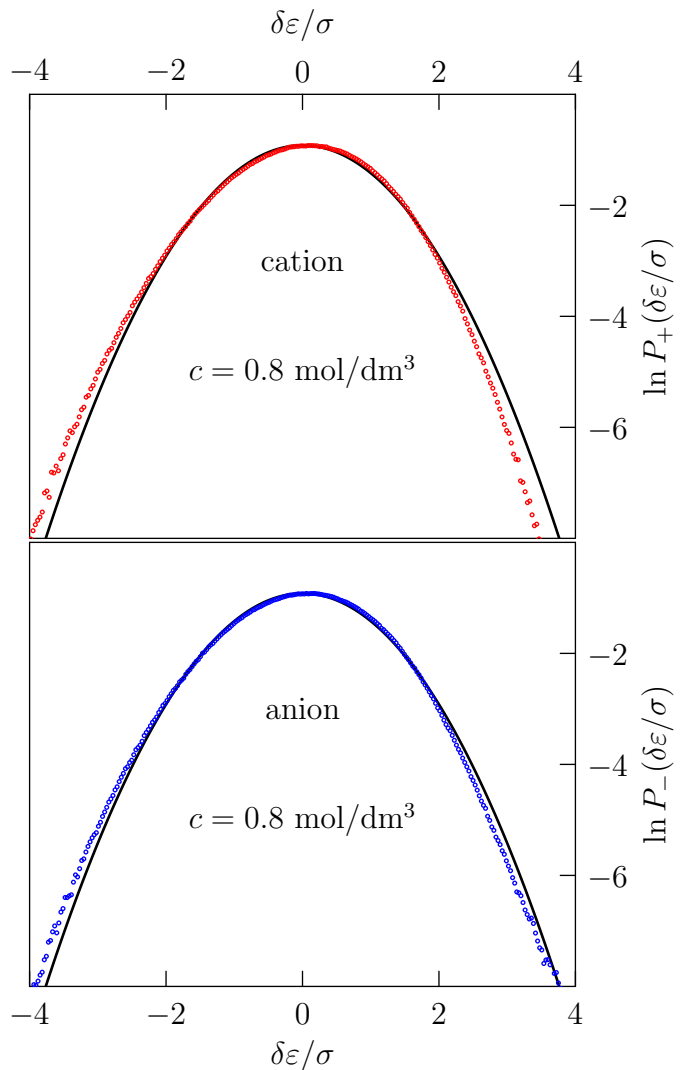


FIG. 3. Observed distributions of ion binding energies, shifted and scaled into standard normal form, for $c = 0.8$ mol/dm³. The parabolae (solid black lines) here are standard normal comparisons.

primitive model considered here.

A. Binding energy distributions

We evaluate binding energies for the primitive model by standard Ewald calculation for configurations extracted from the Monte Carlo simulations, $\epsilon = \Delta W_A^{(1)}$. We examine the distributions of binding energies for the ions present in the simulation, $P(\epsilon)$, and also binding energies for permissible trial placements of additional anions or cations, $P^{(0)}(\epsilon)$. In order to have a basis for comparison, we do these calculations first *without* the conditioning prescribed by QCT, *i.e.*, all anions or cations without regard to their neighborhood status. Distributions of those binding energies (Figs. 3, 4, 5, and 6) are

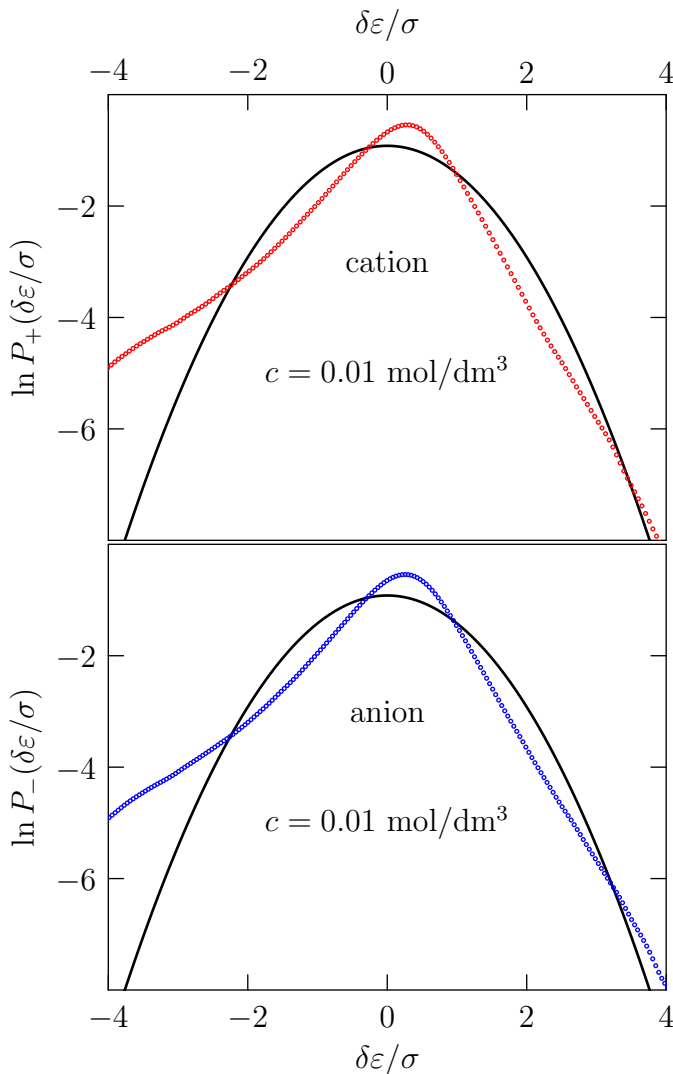


FIG. 4. Observed distributions of ion binding energies, shifted and scaled into standard normal form, for $c = 0.01 \text{ mol/dm}^3$. The parabolae (solid black lines) here are standard normal comparisons.

striking. At the higher concentration shown (Fig. 3), the distributions are reasonably normal as expected. At the lower concentration shown (Fig. 4), the distributions are non-gaussian. The design of the model to reflect ion-pairing is evident in the enhanced weight at substantially negative binding energies.

The normal presentation (as in Figs. 3, 4, and 5, shift-scaled and compared to standard normal) helps to judge the width of these distributions. An alternative presentation (Figs. 8 and 9) compares these binding energy ranges to the thermal energy kT and gives additional insight. The free energy prediction from the coupled distributions (Figs. 3, 4) depends sensitively on the high- ε (right) wing of these graphs and hardly at all on the low- ε (left) wing. Even though the low-concentration distribution (Fig. 4) is strikingly non-gaussian, the right-wing

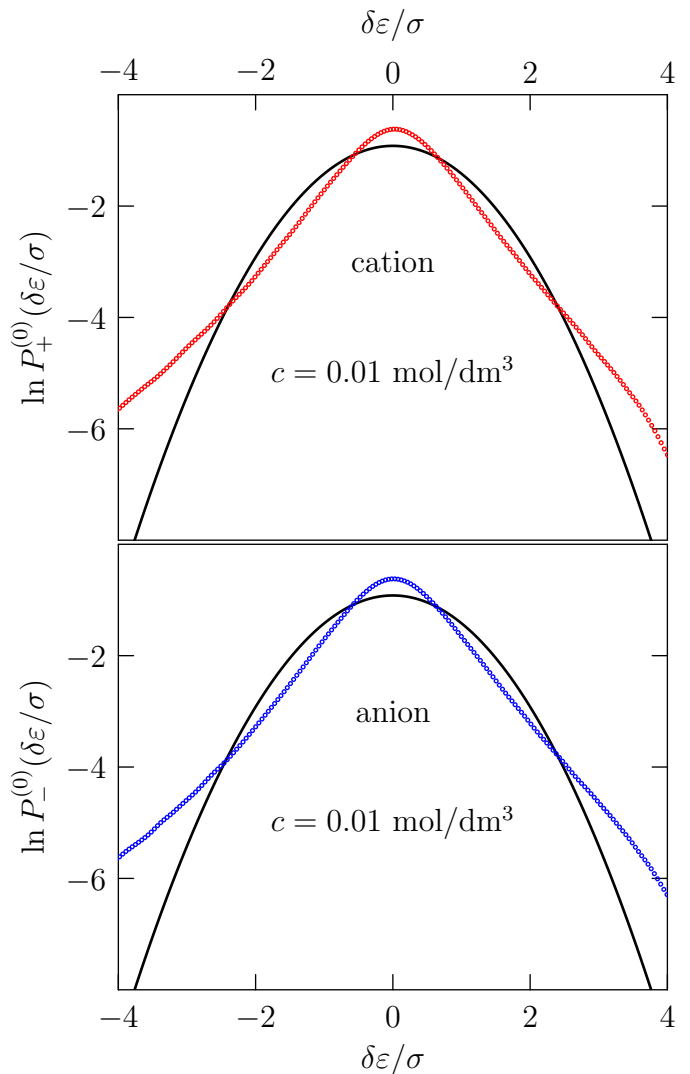


FIG. 5. Observed distributions of uncoupled ion binding energies, shifted and scaled into standard normal form, for $c = 0.01 \text{ mol/dm}^3$. The parabolae (solid black lines) here are standard normal comparisons.

extends, very roughly, to the same width as the natural gaussian. In contrast the uncoupled $P^{(0)}(\varepsilon)$ (Fig. 5) is qualitatively non-gaussian in both high- ε and low- ε wings.

The uncoupled $P^{(0)}(\varepsilon)$ (Figs. 5) at low concentration also distinctly abnormal, in both wings; at high-concentration they (Fig. 6) more nearly gaussian.

B. QCT conditioned binding energy distributions

We next consider the conditioned distributions that arise with the QCT approach (Eq. (11) and Fig. 1). We take the inner-shell to be a sphere of radius λ centered on the ions. Typical results for $P_{-}(\delta\varepsilon/\sigma|n_{\lambda} = 0)$ for the interesting low concentration case (Fig. 7) shows how the

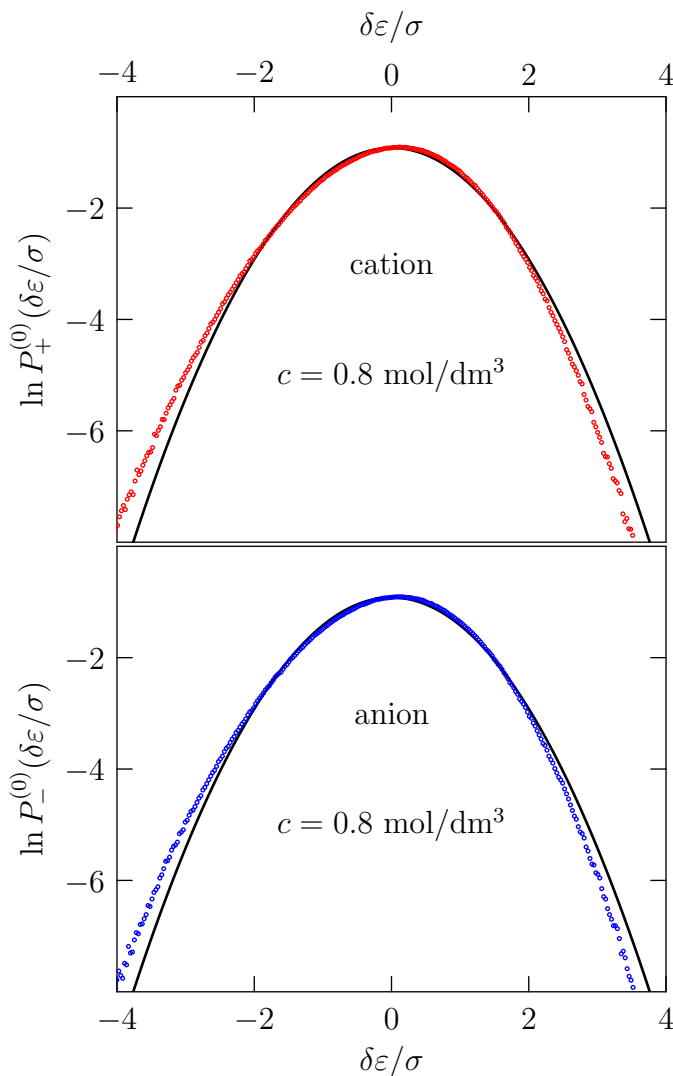


FIG. 6. Observed distributions of uncoupled ion binding energies, shifted and scaled into standard normal form, for $c = 0.8 \text{ mol/dm}^3$. The parabolae (solid black lines) here are standard normal comparisons.

conditioning affects this distribution, with increasing λ driving the distribution toward normal behavior.

C. Free energies and gaussian approximations

The goal of our QCT development is to break the free energy into parts associated first with simple observations, and finally with a partition function calculation (the *outer-shell* contribution) that can be well approximated by a gaussian model with simply observed parameters. In that case the *outer-shell* contribution of Eq. (11)

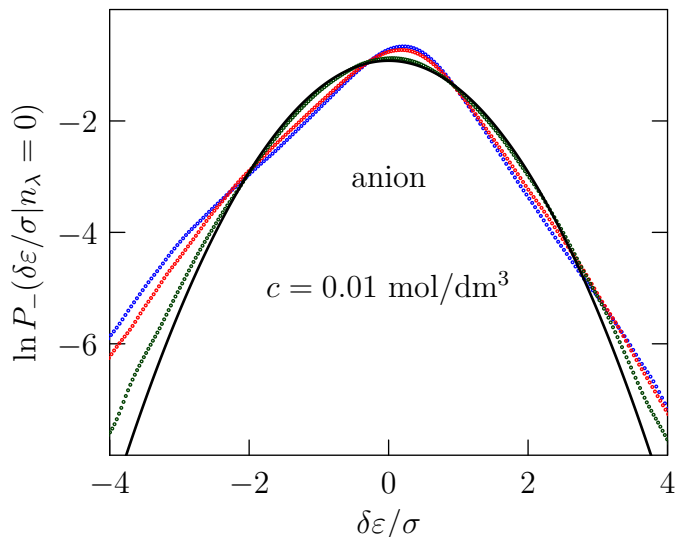


FIG. 7. Probability density functions for the outer-shell binding energy for the anions in the simulation of Table I, for the lowest concentration there, with $\lambda = 0.7, 0.9,$ and 2.0 nm (blue, red, and darkgreen respectively), compared the standard normal (solid black curve). This demonstrates how increasing λ enforces better Gaussian behavior for this distribution.

would be

$$\ln \int e^{\beta \varepsilon} P_A(\varepsilon | \chi_A = 1) d\varepsilon \approx \beta \langle \varepsilon | \chi_A = 1 \rangle + \beta^2 \langle \delta \varepsilon^2 | \chi_A = 1 \rangle / 2. \quad (13)$$

To test these ideas, we evaluate the free energies directly, with and without the QCT conditioning, and also compare the results of the gaussian approximation Eq. (13).

The direct evaluation of the free energies follows Bennett's method,¹⁸ and searches for the value $\Delta\mu^{(\text{ex})}$ that solves

$$\left\langle \frac{1}{1 + e^{-\beta(\varepsilon - \Delta\mu^{(\text{ex})})}} \right\rangle = \left\langle \frac{1}{1 + e^{\beta(\varepsilon - \Delta\mu^{(\text{ex})})}} \right\rangle_0 \quad (14)$$

for each species considered. The average on the left is estimated with the sample associated with $P_A(\varepsilon)$ whereas the average on the right of uses the binding energies leading to $P_A^{(0)}(\varepsilon)$ associated with permissible trial placements.

1. No conditioning

In this case, we estimate a non-electrostatic contribution directly by trial insertions, then electrostatic contribution on the basis of distributions such as Figs. 4 and 5. The mean activity coefficients (Fig. 10) obtained with the gaussian approximation and the Bennett evaluation are qualitatively similar but quantitatively different from each other.

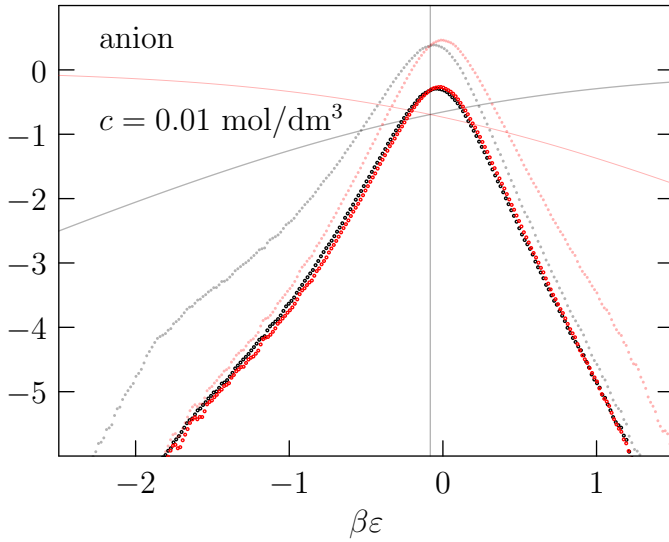


FIG. 8. For the low concentration case of Table I. The bold circles are the logarithms of the functions left and right of Eq. (15), black and red, respectively. The pale solid curves are the corresponding weight factors, *e.g.* $-\ln \left[1 + e^{\beta(\varepsilon - \Delta\mu_{\alpha}^{(ex)})} \right]$ for the red curve. The pale symbols are the plotted logarithms of the observed probability densities. The vertical line is the inferred value of the $\beta\Delta\mu_{\alpha}^{(ex)}$. Note the Eq. (15) is accurately satisfied.

2. Pointwise Bennett comparison

A more specific statement of the Bennett approach is

$$\frac{P(\varepsilon)}{1 + e^{-\beta(\varepsilon - \Delta\mu^{(ex)})}} = \frac{P^{(0)}(\varepsilon)}{1 + e^{\beta(\varepsilon - \Delta\mu^{(ex)})}}. \quad (15)$$

This relies on the basic relation

$$P(\varepsilon) = e^{-\beta(\varepsilon - \Delta\mu^{(ex)})} P^{(0)}(\varepsilon), \quad (16)$$

and the elementary identity

$$e^{-\beta(\varepsilon - \Delta\mu^{(ex)})} = \frac{1 + e^{-\beta(\varepsilon - \Delta\mu^{(ex)})}}{1 + e^{\beta(\varepsilon - \Delta\mu^{(ex)})}}. \quad (17)$$

Eq. (15) assembles information from $P(\varepsilon)$ and $P^{(0)}(\varepsilon)$, and thus illuminates the behavior of the important wings, high- ε for $P(\varepsilon)$ and low- ε for $P^{(0)}(\varepsilon)$. Typical results (Figs. 8 and 9) show reasonable match between the left and right side of Eq. (15). It is helpful to note that at the higher concentration shown (Fig. 9), the match in the low-probability wings is not perfect. A reasonable guess is that this is due to inaccuracy of $P^{(0)}(\varepsilon)$ at low- ε and that this is the reason behind the puzzling discrepancy between the Bennett result and the gaussian model seen in Figs. 10 and 13.

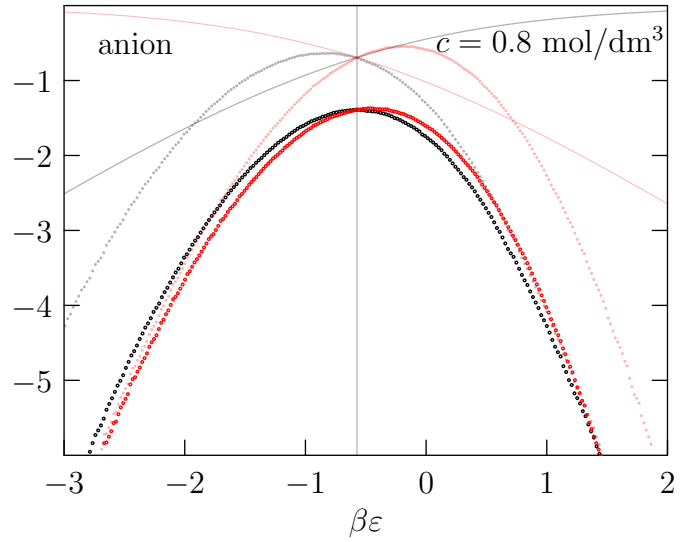


FIG. 9. For the $c=0.8 \text{ mol/dm}^3$ case of Table I. The bold circles are the logarithms of the functions left and right of Eq. (15), black and red, respectively. The pale solid curves are the corresponding weight factors, *e.g.* $-\ln \left[1 + e^{-\beta(\varepsilon - \Delta\mu_{\alpha}^{(ex)})} \right]$ for the black curve. The pale symbols are the plotted logarithms of the observed probability densities. The vertical line is the inferred value of the $\beta\Delta\mu_{\alpha}^{(ex)}$. Note the Eq. (15) is only roughly satisfied in the low- ε wing.

3. QCT conditioning

Though the various QCT contributions depend on the radius λ of the inner-shell (Fig. 11), the net free energy varies only slightly with increases of $\lambda > 0.7 \text{ nm}$. The mean activity coefficients evaluated by the Bennett method and the gaussian approximation (Fig. 13) now accurately agree. This suggests that both approaches are physically reliable with this conditioning. In order that an MM pair-potential at long-range may be plausibly exploited, the conditioning is essential to the broader idea here.

For the concentrations and λ values in Fig. 11, the Poisson estimates of the packing and chemical contributions¹⁵

$$\begin{aligned} -\ln \langle \langle \chi \rangle \rangle_0 &\equiv -\sum_{\alpha} \ln \langle \langle \chi_{\alpha} \rangle \rangle_0 \\ &= \left(\frac{1}{2} \right) \sum_{\alpha, \gamma} \frac{4\pi}{3} \lambda^3 c, \quad (18) \end{aligned}$$

$$\begin{aligned} -\ln \langle \chi \rangle &\equiv -\sum_{\alpha} \ln \langle \chi_{\alpha} \rangle \\ &= \left(\frac{1}{2} \right) \sum_{\alpha, \gamma} 4\pi \int_0^{\lambda} c g_{\alpha\gamma}(r) r^2 dr, \quad (19) \end{aligned}$$

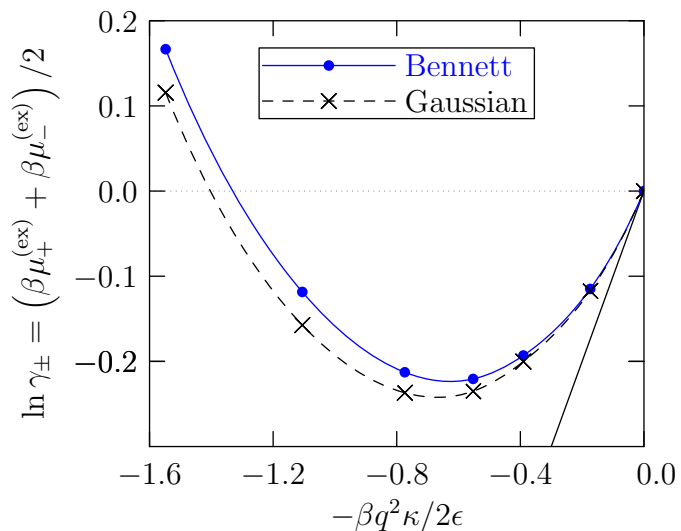


FIG. 10. No conditioning, non-QCT, as discussed in Sec. III C 1. The solid black line is the Debye-Hückel limiting law.

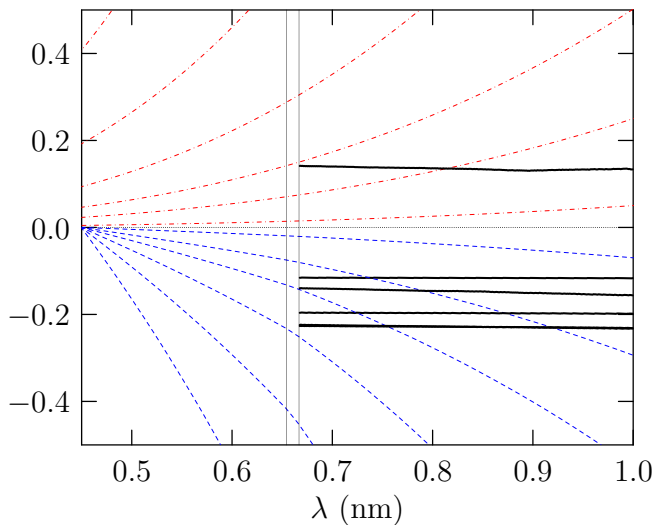


FIG. 11. The red, blue, and black curves are the packing (arithmetic average of $-\ln \langle \chi \rangle_0$ for the two ion types), chemical (arithmetic average of $\ln \langle \chi \rangle$ for the two ion types), and net contributions (following Eq. (11), including the outer-shell contribution, for $\ln \gamma_{\pm}$), respectively, for the primitive model results.¹⁵ The various curves correspond to $c = \{0.01, 0.05, 0.1, 0.2, 0.4, 0.8\}$ mol/dm³ cases of Table I.

are useful. The combination

$$-\ln \left[\frac{\langle \langle \chi \rangle_0 \rangle}{\langle \chi \rangle} \right] = - \left(\frac{1}{2} \right) \sum_{\alpha, \gamma} 4\pi \int_0^\lambda c [g_{\alpha\gamma}(r) - 1] r^2 dr. \quad (20)$$

is then interesting. The utility of these results emphasize again that the ion densities are not high, so simple results can be helpful.

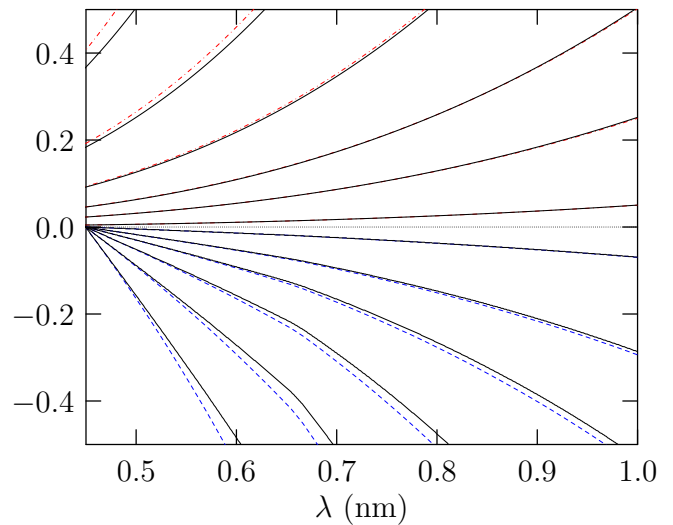


FIG. 12. Upper black curves are the results from Eq. (18). Similarly, the red dot-dashed curves are the direct numerical results obtained by trail insertions. The lower black are the results from Eq. (19). Similarly, the blue dashed curves are the direct numerical results obtained by observations of the ions present in the simulations.

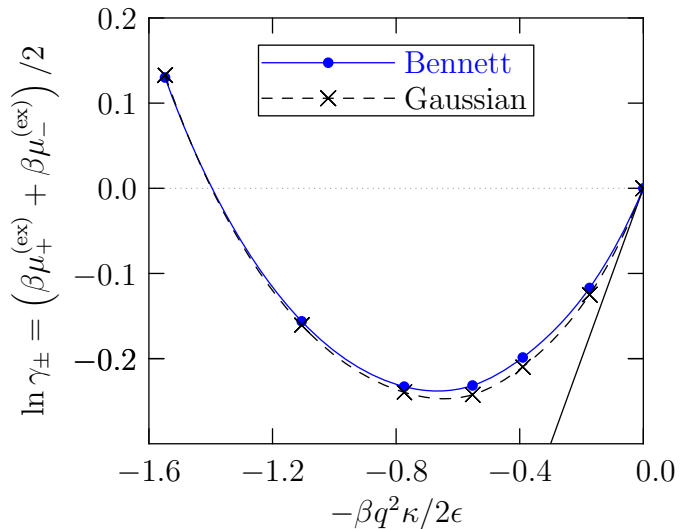


FIG. 13. QCT, as discussed in Sec. II C. The solid black line is the Debye-Hückel limiting law.

IV. CONCLUSIONS

This paper organizes several basic theoretical results — McMillan-Mayer theory, the potential distribution approach, and quasi-chemical theory — to apply high-resolution AIMD to electrolyte solutions. The conceptual target for these considerations is that the last of the calculations depicted in Fig. 1 can be done by AIMD directly on the time and space scales typical of those demanding methods. This theory then develops a mechanism for addressing effects associated with longer spatial

scales, involving also characteristically longer time scales. The theory treats composition fluctuations which would be accessed by larger-scale calculations, and also longer-ranged interactions and correlations that are of special interest for electrolyte solutions.

The quasi-chemical organization, as an extension of van der Waals pictures, breaks-up governing free energies into physically distinct contributions: *packing*, *outer-shell*, and *chemical* contributions. This paper adopted a primitive model suggested by observed ion-pairing in tetra-ethylammonium tetra-fluoroborate dissolved in propylene carbonate, then studied specifically the *outer-shell* contributions that expresses electrolyte screening. Gaussian statistical models are shown to be effective as physical models for these *outer-shell* contributions, and they are conclusive for the free energies within the quasi-chemical formulation (Figs. 11 and 13). In fact, with this data set the gaussian physical approximation is more efficient in providing an accurate mean activity coefficient than is the Bennett direct evaluation of that free energy (Figs. 10 and 13).

V. ACKNOWLEDGEMENTS

This work was supported by the National Science Foundation under the NSF EPSCoR Cooperative Agreement No. EPS-1003897, with additional support from the Louisiana Board of Regents.

APPENDIX A: ACCESSIBLE DERIVATION OF THE MCMILLAN-MAYER THEORY

In the analysis of the MM theory, the formulae that are employed can be intimidating¹⁹⁻²¹ at several stages so a physically clear notation helps. We consider a system composed of solvent (S) and solutes (A). The numbers of these species will be indicated by \mathbf{n}_S and \mathbf{n}_A , the bold-face typography indicating that each of these quantities can be multi-component, *i.e.*, $\mathbf{n}_A = \{n_{A_1}, n_{A_2}, \dots\}$, and similarly for solvent species. The Helmholtz free energy $A(T, V, \mathbf{n}_S, \mathbf{n}_A)$ then leads to the canonical partition function

$$e^{-\beta A(T, V, \mathbf{n}_S, \mathbf{n}_A)} = \mathcal{Q}(\mathbf{n}_S, \mathbf{n}_A) / (\mathbf{n}_S! \mathbf{n}_A!) . \quad (\text{A-1})$$

T (temperature) and V (volume) have their usual meanings, and we will suppress that notation on the right of Eq. (A-1). To further fix the notation we recall²² $\mathcal{Q}(n_A = 1) \equiv V q_A^{(\text{int})} / \Lambda_A^3$ is the canonical ensemble partition function for a system comprising exactly one molecule of type A in a volume V with Λ_A is the thermal deBroglie wavelength. The factorial notation

$$\mathbf{n}_A! = n_{A_1}! n_{A_2}! \dots \quad (\text{A-2})$$

is common.^{19,22} When convenient, we will denote $\mathbf{n} = \{\mathbf{n}_S, \mathbf{n}_A\}$ so that

$$e^{-\beta A(T, V, \mathbf{n})} = \mathcal{Q}(\mathbf{n}) / \mathbf{n}! . \quad (\text{A-3})$$

The grand canonical partition function will be central,

$$e^{\beta p V} = \sum_{\mathbf{n} \geq 0} \mathcal{Q}(\mathbf{n}) \left(\frac{\mathbf{z}^{\mathbf{n}}}{\mathbf{n}!} \right) , \quad (\text{A-4})$$

in these terms. Here we adopt a correspondingly simplified notation for the activities^{19,22}

$$\mathbf{z}^{\mathbf{n}} = \exp \left\{ \sum_X \beta \mu_X n_X \right\} \quad (\text{A-5})$$

with μ_X the chemical potential of species X. We will compare the pressure of the solution with the pressure of the solvent-only system at the same activity $z_S = e^{\beta \mu_S}$:

$$e^{\beta(p-\pi)V} = \sum_{\mathbf{n}_S \geq 0} \mathcal{Q}(\mathbf{n}_S, \mathbf{n}_A = 0) \left(\frac{z_S^{\mathbf{n}_S}}{\mathbf{n}_S!} \right) . \quad (\text{A-6})$$

The pressure difference π is the osmotic pressure. The probability for observing \mathbf{n}_S in the solvent-only system is

$$P(\mathbf{n}_S; \mathbf{z}_A = 0) = \mathcal{Q}(\mathbf{n}_S, \mathbf{n}_A = 0) \left(\frac{z_S^{\mathbf{n}_S}}{\mathbf{n}_S!} \right) \times e^{-\beta(p-\pi)V} . \quad (\text{A-7})$$

With these notations we write

$$\begin{aligned} e^{\beta \pi V} &= \\ \sum_{\mathbf{n}_A \geq 0} \left(\frac{\mathbf{z}_A^{\mathbf{n}_A}}{\mathbf{n}_A!} \right) \sum_{\mathbf{n}_S \geq 0} \left\{ \frac{\mathcal{Q}(\mathbf{n}_S, \mathbf{n}_A)}{\mathcal{Q}(\mathbf{n}_S, \mathbf{n}_A = 0)} \right\} P(\mathbf{n}_S; \mathbf{z}_A = 0) \\ &= \sum_{\mathbf{n}_A \geq 0} \mathcal{Z}(\mathbf{n}_A; \mathbf{z}_S) \left(\frac{\mathbf{z}_A^{\mathbf{n}_A}}{\mathbf{n}_A!} \right) . \end{aligned} \quad (\text{A-8})$$

The important point is the structural similarity to Eq. (A-4).

Our task is to analyze the MM configurational integral

$$\begin{aligned} \mathcal{Z}(\mathbf{n}_A; \mathbf{z}_S) &= \\ \sum_{\mathbf{n}_S \geq 0} \left\{ \frac{\mathcal{Q}(\mathbf{n}_S, \mathbf{n}_A)}{\mathcal{Q}(\mathbf{n}_S, \mathbf{n}_A = 0)} \right\} P(\mathbf{n}_S; \mathbf{z}_A = 0) \end{aligned} \quad (\text{A-9})$$

The displayed ratio of partition functions is distinctive. For the case $\mathbf{n}_A = 1$, for example, we write

$$\begin{aligned} \sum_{\mathbf{n}_S \geq 0} \left\{ \frac{\mathcal{Q}(\mathbf{n}_S, \mathbf{n}_A = 1)}{\mathcal{Q}(\mathbf{n}_S, \mathbf{n}_A = 0)} \right\} P(\mathbf{n}_S; \mathbf{z}_A = 0) \\ = \mathcal{Q}(\mathbf{n}_S = 0, \mathbf{n}_A = 1) \left\langle \left\langle e^{-\beta \Delta U_A^{(1)}} \right\rangle \right\rangle_0 , \end{aligned} \quad (\text{A-10})$$

where the right-most factor is to be evaluated at infinite dilution of the solute, $\mathbf{z}_A = 0$. The potential distribution development establishes that right-side to be²²

$$\begin{aligned} \mathcal{Q}(\mathbf{n}_S = 0, \mathbf{n}_A = 1) \left\langle \left\langle e^{-\beta \Delta U_A^{(1)}} \right\rangle \right\rangle_0 \\ = \lim_{z_A \rightarrow 0} \left(\frac{n_A}{z_A} \right) = \lim_{z_A \rightarrow 0} \left(\frac{\rho_A}{z_A} \right) V . \end{aligned} \quad (\text{A-11})$$

To write the general term for Eq. (A-9), we will use

$$\binom{\mathbf{n}_A}{\mathbf{m}_A}$$

to denote the number of ways of selecting the \mathbf{m}_A solute molecule set from the collection \mathbf{n}_A . For example, if only one type of solute A is considered, then

$$\binom{n_A}{m_A} = \frac{n_A!}{m_A!(n_A - m_A)!} = \frac{n_A^{m_A}}{m_A!}, \quad (\text{A-12})$$

as usual, with the last equality using the ‘ n_A -to-the- m_A -falling’ notation.^{22,23}

For more general but specified \mathbf{m}_A , we rewrite Eq. (A-9)

$$\sum_{\mathbf{n}_S \geq 0} \left\{ \frac{\mathcal{Q}(\mathbf{n}_S, \mathbf{m}_A)}{\mathcal{Q}(\mathbf{n}_S, \mathbf{m}_A = 0)} \right\} P(\mathbf{n}_S; z_A = 0) \\ = \mathcal{Q}(\mathbf{n}_S = 0, \mathbf{m}_A) \left\langle \left\langle e^{-\beta \Delta U(\mathbf{m}_A)} \right\rangle \right\rangle_0 \quad (\text{A-13})$$

and again, after having set \mathbf{m}_A , this is to be evaluated at infinite dilution. Here the binding energy

$$\Delta U(\mathbf{m}_A) = U(\mathbf{n}_S, \mathbf{m}_A) \\ - U(\mathbf{n}_S, \mathbf{m}_A = 0) - U(\mathbf{n}_S = 0, \mathbf{m}_A), \quad (\text{A-14})$$

is associated with the collection of \mathbf{m}_A solute molecules. Following the potential distribution theory further²²

$$\mathcal{Q}(\mathbf{n}_S = 0, \mathbf{m}_A) \left\langle \left\langle e^{-\beta \Delta U(\mathbf{m}_A)} \right\rangle \right\rangle_0 \\ = \left\langle \left\langle \binom{\mathbf{n}_A}{\mathbf{m}_A} \right\rangle \right\rangle \frac{m_A!}{z_A^{m_A}}, \quad (\text{A-15})$$

Finally,

$$\left\langle \left\langle \binom{\mathbf{n}_A}{\mathbf{m}_A} \right\rangle \right\rangle m_A! \\ = \rho_A^{m_A} \int_V d1_A \dots \int_V dm_A g(\mathbf{m}_A) (1_A \dots m_A), \quad (\text{A-16})$$

with $g(\mathbf{m}_A) (1_A \dots m_A)$ denoting the usual \mathbf{m}_A joint distribution function. Here we denote solute configurational coordinates as $(1_A, \dots, m_A)$, and the necessary integrations by $\int_V d1_A \dots \int_V dm_A$. This produces the factor of V in Eq. (A-11). Since we wish to simplify Eq. (A-13),

with $z_A = 0$, we use Eq. (A-15) to write

$$\mathcal{Z}(\mathbf{n}_A; z_S) = \left[\lim_{z_A \rightarrow 0} \left(\frac{\rho_A}{z_A} \right) \right]^{\mathbf{n}_A} \\ \int_V d1_A \dots \int_V dn_A g(\mathbf{n}_A) (1_A \dots n_A; z_A = 0) \quad (\text{A-17})$$

The prefactor, to be evaluated at infinite dilution, is given by

$$\frac{\rho_A}{z_A} = \frac{q_A^{\text{int}}}{\Lambda_A^3} \left\langle \left\langle e^{-\beta \Delta U_A^{(1)}} \right\rangle \right\rangle_0 \quad (\text{A-18})$$

in the potential distribution theorem formulation.²²

With this suggestive form we can be more specific about the canonical configurational integrals that started our discussion, specifically

$$\mathcal{Q}(\mathbf{n}_A) = \lim_{z_S \rightarrow 0} \mathcal{Z}(\mathbf{n}_A; z_S) \\ = \lim_{z_S \rightarrow 0} \left[\lim_{z_A \rightarrow 0} \left(\frac{\rho_A}{z_A} \right) \right]^{\mathbf{n}_A} \\ \times \int_V d1_A \dots \int_V dn_A e^{-\beta W(1_A \dots n_A)}. \quad (\text{A-19})$$

The multipliers appearing on the middle line supply features of the kinetic energy portion of the partition function, specific to the implementation for the particular case. For notational simplicity we will drop the specific identification of the solvent activity in the formulae elsewhere.

These formulae, particularly Eq. (A-19), are collected in the summary statement of MM theory in Sec. II A, and particularly with Eq. (2).

APPENDIX B: POTENTIAL DISTRIBUTION THEORY

With the MM background, we evaluate the average number of solute A molecules as

$$\langle n_A \rangle = e^{-\beta \pi V} \sum_{\mathbf{n}_A \geq 0} n_A \mathcal{Z}(\mathbf{n}_A; z_S) \left(\frac{z_A^{n_A}}{n_A!} \right). \quad (\text{B-1})$$

Since the summand factor n_A annuls the $n_A = 0$ term, this result presents an explicit leading factor of z_A . Determination of z_A establishes the thermodynamic property μ_A . Therefore, we rewrite this equation by bringing forward the explicit extra factor of z_A as

$$\langle n_A \rangle = e^{-\beta \pi V} \mathcal{Z}(\mathbf{n}_A = 1; z_S) z_A \sum_{\mathbf{n}_A \geq 0} \left(\frac{\mathcal{Z}(\mathbf{n}_A + 1; z_S)}{\mathcal{Z}(\mathbf{n}_A = 1; z_S) \mathcal{Z}(\mathbf{n}_A; z_S)} \right) \mathcal{Z}(\mathbf{n}_A; z_S) \left(\frac{z_A^{n_A}}{n_A!} \right). \quad (\text{B-2})$$

or

$$\langle n_A \rangle = \mathcal{Z}(\mathbf{n}_A = 1; z_S) z_A \left\langle \left\langle e^{-\beta \Delta W_A^{(1)}} \right\rangle \right\rangle_0. \quad (\text{B-3})$$

Here

$$\Delta W_A^{(1)} = W(\mathbf{n}_A + 1) - W(\mathbf{n}_A) - W(1), \quad (\text{B-4})$$

is the binding energy of a distinguished solute (A) molecule in the MM system, and the quantity

$$\mathcal{Z}(n_A = 1; z_S) = \frac{Vq_A^{(\text{int})}}{\Lambda_A^3} \left\langle \left\langle e^{-\beta\Delta U_A^{(1)}} \right\rangle \right\rangle_0 \quad (\text{B-5})$$

involves interactions of one A molecule and the solvent; it is proportional to the system volume.

APPENDIX C: QCT BREAKUP IN THE GRAND CANONICAL ENSEMBLE

Here we discuss twists associated with the consideration of PDT developments when n_A fluctuates. We begin with the observation from Eq. (B-3) that

$$\left\langle \left\langle e^{-\beta\Delta W_A^{(1)}} \right\rangle \right\rangle_0 \propto \langle n_A \rangle. \quad (\text{C-1})$$

Then considering the ratio

$$\frac{\left\langle \left\langle e^{-\beta\Delta W_A^{(1)}} F \right\rangle \right\rangle_0}{\left\langle \left\langle e^{-\beta\Delta W_A^{(1)}} \right\rangle \right\rangle_0} = \frac{\langle F n_A \rangle}{\langle n_A \rangle}, \quad (\text{C-2})$$

yields a particularly transparent result. Choosing $F = e^{\beta\Delta W_A^{(1)}} \chi_A$, we obtain an analogue of Eq (8):

$$\frac{\left\langle e^{\beta\Delta W_A^{(1)}} \chi_A n_A \right\rangle}{\langle n_A \rangle} = \frac{\langle \langle \chi_A \rangle \rangle_0}{\left\langle \left\langle e^{-\beta\Delta W_A^{(1)}} \right\rangle \right\rangle_0}. \quad (\text{C-3})$$

If the averages are canonical then this is just Eq (8) again, but Eq. (C-3) remains true if n_A fluctuates.

We expect that

$$\frac{\left\langle e^{\beta\Delta W_A^{(1)}} \chi_A n_A \right\rangle}{\langle n_A \rangle} \sim \left\langle e^{\beta\Delta W_A^{(1)}} \chi_A \right\rangle + O(\langle n_A \rangle^{-1}), \quad (\text{C-4})$$

so in the thermodynamic limit that average matches the simpler canonical expression. The physical reason for this expectation is that we can write $n_A = \langle n_A \rangle + \delta n_A$ in the numerator. Then the correlation of δn_A with the intensive characteristic of that numerator average should yield an intensive result.

Accepting this argument for the moment and retaining only the dominant contribution in Eq. (C-4), we recover the results of Sec. II C — and specifically the important result Eq. (11) — but consistently with the grand canonical ensemble derivation of the earlier sections.

To make that physical view specific, we introduce the additional notation

$$\left\langle e^{\beta\Delta W_A^{(1)}} | n_A \right\rangle$$

for the canonical ensemble average that specifies n_A . For anticipated δn_A , we use

$$\left\langle e^{\beta\Delta W_A^{(1)}} \chi_A | n_A \right\rangle \approx \left\langle e^{\beta\Delta W_A^{(1)}} \chi_A | \langle n_A \rangle \right\rangle + \delta n_A \left(\frac{\partial \left\langle e^{\beta\Delta W_A^{(1)}} \chi_A | \langle n_A \rangle \right\rangle}{\partial \langle n_A \rangle} \right). \quad (\text{C-5})$$

Used in the left-side of Eq. (C-4), and then averaging with respect to n_A occupancies, this yields

$$\frac{\left\langle e^{\beta\Delta W_A^{(1)}} \chi_A n_A \right\rangle}{\langle n_A \rangle} \approx \left\langle e^{\beta\Delta W_A^{(1)}} \chi_A | \langle n_A \rangle \right\rangle + \frac{\langle \delta n_A^2 \rangle}{\langle n_A \rangle} \left(\frac{\partial \left\langle e^{\beta\Delta W_A^{(1)}} \chi_A | \langle n_A \rangle \right\rangle}{\partial \langle n_A \rangle} \right), \quad (\text{C-6})$$

the expected result. Since

$$\langle \delta n_A^2 \rangle = \left(\frac{\partial \langle n_A \rangle}{\partial \beta \mu_A} \right)_{T, V, \mu_S},$$

the correction indeed vanishes in the thermodynamic limit.

- ¹L. Yang, B. H. Fishbine, A. Migliori, and L. R. Pratt, *J. Chem. Phys.* **132**, 044701(1) (2010).
- ²S. K. Ma, *Modern Theory of Critical Phenomena* (W. A. Benjamin, Inc, Reading, MA, 1976).
- ³H. L. Friedman and W. D. T. Dale, in *STATISTICAL MECHANICS PART A: EQUILIBRIUM TECHNIQUES*, edited by B. J. Berne (Plenum, New York, 1977) pp. 85–136.
- ⁴H. L. Friedman, *Ann. Rev. Phys. Chem.* **32**, 1798 (1981).
- ⁵W. G. McMillan Jr and J. E. Mayer, *J. Chem. Phys.* **13**, 276 (1945).
- ⁶T. L. Hill, *STATISTICAL THERMODYNAMICS* (Addison-Wesley, Reading, MA USA, 1960) Chap. SS19.1.
- ⁷S. A. Adelman, *Chem. Phys. Letts.* **38**, 567 (1976).
- ⁸P. G. Kusalik and G. N. Patey, *J. Chem. Phys.* **89**, 7478 (1988).
- ⁹C. P. Ursenbach, D. Wei, and G. N. Patey, *J. Chem. Phys.* **94**, 6782 (1991).
- ¹⁰D. Asthagiri, P. D. Dixit, S. Merchant, M. E. Paulaitis, L. R. Pratt, S. B. Rempe, and S. Varma, *Chem. Phys. Letts.* **485**, 1 (2010).
- ¹¹D. Sabo, D. Jiao, S. Varma, L. R. Pratt, and S. B. Rempe, *Annu. Rep. Prog. Chem. Soc. C* (2013).
- ¹²B. Widom, *Science* **157**, 375 (1967).
- ¹³D. Chandler, J. D. Weeks, and H. C. Andersen, *Science* **220**, 787 (1983).
- ¹⁴D. M. Rogers, D. Jiao, L. R. Pratt, and S. B. Rempe, *Ann. Rep. Comp. Chem.* **8**, 71 (2012).
- ¹⁵P. Zhu, X. You, L. R. Pratt, and K. D. Papadopoulos, *J. Chem. Phys.* **134**, 054502 (2011).
- ¹⁶P. Zhu, L. R. Pratt, and K. D. Papadopoulos, *J. Chem. Phys.* **137**, 174501 (2012).
- ¹⁷M. G. Martin, “Towhee,” Tech. Rep. (2010) <http://sourceforge.net/projects/towhee/>.
- ¹⁸C. H. Bennett, *J. Comp. Phys.* **22**, 245 (1976).
- ¹⁹J. E. Mayer and M. G. Mayer, *Statistical Mechanics*, 2nd ed. (Wiley-Interscience, 1977).
- ²⁰A. Münster, *Statistical Thermodynamics*, Vol. 2 (Academic Press, New York, 1974).
- ²¹H. L. Friedman, *Ionic Solution Theory* (Interscience, 1962).
- ²²T. L. Beck, M. E. Paulaitis, and L. R. Pratt, *THE POTENTIAL DISTRIBUTION THEOREM AND MODELS OF MOLECULAR SOLUTIONS* (Cambridge University Press, 2006).
- ²³R. L. Graham, D. E. Knuth, and O. Patashnik, *Concrete Mathematics* (Addison-Wesley, 1989).